Eur J Med Res (2006) 11: 471-478

Analysis of Biodegradation of Copolymer Dermis Substitutes in the Dorsal Skinfold Chamber of balb/c Mice

A. Ring[1], O. Goertz[2], L. Steinstraesser[2], C. Kuhnen[3], I. Schmitz[3], G. Muhr[1], H. U. Steinau[2], S. Langer[2]

[1]Department of Surgery, Trauma Center (Director: Prof. Dr. med. G. Muhr),
[2]Department of Plastic and Hand Surgery, Burn Center (Director: Prof. Dr. med. H.-U. Steinau),
[3]Department of Pathology (Director: Prof. Dr. med. A. Tannapfel),
University Hospital Bergmannsheil, Bochum, Germany

Abstract
PEGT/PBT-block-copolymer dermis substitutes were inserted into dorsal skinfold chambers of balb/c mice (n=36). Scaffolding matrices with 3 different pore diameters (pore diameter: <75μm, 75-212μm and 250-300μm) were analyzed on days 7, 14, and 21 post implantation by scanning electron and light microscopy. The quantification of matrix fragmentation was performed using image-analytical software analySIS®. The fragmentation rate in scaffolding matrices with a pore size of < 75μm was observed to be higher than in matrices of larger pore sizes. Image-analytical evaluation over 21 days revealed a reduction of the copolymer matrix by approximately 32% for the <75μm matrices, 23% for the 75-212μm matrices and 18% for the matrices, where pore size ranged between 250μm and 300μm. Twenty-one days after implantation, the matrix pores of 75-212μm and 250-300μm scaffolds were totally filled by vascularized fibrous tissue. Contrarily, an increased formation of foreign-body giant cells was observed in matrices with pore size <75μm.

The pore size of the scaffolding PEGT/PBT dermis substitutes affects their degradative behaviour in vivo.

Key words: PEGT/PBT, biopolymer, three-dimensional scaffold, biodegradation, dermis substitute, skinfold chamber, microcirculation

Introduction

The loss of tissue due to trauma and wound infection is one of the frequent and expensive problems in human health care today. It is expected that the techniques to regenerate human tissue by tissue engineering will have an important influence on the wound treatment and clinical outcome of patients with extensive tissue defects [1, 2]. Reconstructive surgery would benefit in particular from tissue engineering by the application of artificially engineered tissue.

Synthetic three-dimensional biopolymer matrices are used as scaffolds for tissue regeneration. Development of biocompatible and biodegradable scaffolds for neodermal tissue regeneration is presently the subject of several research projects on artificial dermis substitutes. A successful application of bioengineered tissue constructs is dependent on the many characteristics of their supporting synthetic matrix. An appropriate pore geometry (porosity, pore size and interconnectivity of pores) was shown to determine the rate of tissue ingrowth, amount of extracellular matrix deposition and cell survival in the porous biomaterials [3-7].

One of the prerequisites for using biopolymer matrices as dermis substitutes is the ability to allow optimal infiltration of fibrovascular tissue into biomaterial. Furthermore, a controlled reduction or loss of the biomaterial at approximately the same rate as required for replacement by the newly produced dermal matrix is advantageous for the biofunctionality of the artificial substitute.

To quantify the biodegradation of a potential scaffolding dermis substitute in vivo, we implanted the porous PEGT/PBT-block-copolymer matrices of three different pore diameters into the dorsal skinfold chamber of balb/c mice. The matrix degradation was evaluated in relation to the intensity of the host tissue response and the amount of tissue deposition in the pores of the matrix.

The biocompatible PEGT/PBT copolymer belongs to the class of elastomeric segmented polyether/polyester amphiphilic multiblock copolymers [8]. Its hydrophilic polyethylene glycol (PEG) segment is non-toxic and non-immunogenic. PEG is soluble in both organic solvents and water [9]. The hydrophobic blocks of polybutylene terephthalate (PBT) have been used to obtain physically cross-linked biodegradable polymers.

The PEGT/PBT copolymer is expected to break down into its monomers due to chemical hydrolysis of ester bonds when placed in a biological system. Pure aromatic polyesters such as PBT are considered to be highly insensitive to hydrolytic degradation. However, a significant degradation of these polyesters by enzymatic processes could be demonstrated [10]. It was also demonstrated that the loss of copolymer mass and the degradation rate are reduced by increasing the fraction of aromatic components (terephtalic acid) [11, 12].

Several in vitro and in vivo studies showed that PEG/PBT copolymers are biocompatible, well-tolerated and do not cause adverse tissue or systemic reactions [13-17]. This biopolymer has been shown to support adhesion and growth of fibroblasts and ker-

atinocytes and in vivo ingrowth of vascular and connective tissue [18-21].

Materials and Methods

Animals

Female balb/c mice (n=36), weighing 18-22 g were obtained from Charles River, Sulzfeld, Germany. The animals were kept at 21ºC in a 12h light/dark cycle, fed on standard pellets (Spezialdiaeten Soest, Germany) and water ad libitum. The experimental protocol was reviewed and approved by Animal Ethics Committee.

Copolymer Matrices

PEGT/PBT-block-copolymer matrices were obtained from IsoTis NV, Bilthoven, the Netherlands. The biomaterial is a segmented polyether-polyester block-copolymer composed of alternating soft hydrophilic polyethylene glycol terephtalate, and hard hydrophobic polybutylene terephtalate segments. The copolymer composition is indicated as aPEGTbPBTc, where a is the PEG molecular weight, b weight % of PEGT and c the weight % of PBT. Scaffolding matrices with a PEGT/PBT weight ratio of 55/45 and PEGT MW of 300 Da (300PEGT55PBT45) and porosity of 70-80% were used in this study.

PEGT/PBT block copolymers were synthesized by two-step melt polycondensation. Trans-esterification of dimethyl terephthalate with PEG and 1,4-butanediol at approximately 200°C was performed in presence of titaniumbutoxide as a catalyst and α-tocopherol as antioxidant.

Porous structures of matrices were prepared by compression molding of polymer/salt mixtures followed by salt leaching. Matrices were dried under reduced pressure in a vaccum oven, vacuum sealed and sterilized with γ-irradiation [22, 23].

The Technique of the Dorsal Skinfold Chamber

The animals were anesthetized by s.c. injections of 20-25µl of saline solution containing ketamine (Ketavet 100mg/ml, Pharmacija & Upjohn, Erlangen, Germany) and xylazine (Rompun 2%, Bayer Vital, Leverkusen, Germany). The implantation field on the mouse's back was shaved, chemically depilated (Pilca Med, Olivia, Hamburg, Germany) and cleaned with 70% alcohol. Using an operation stereo-microscope (Leica Microsystems, Bensheim, Germany) and microsurgical instruments (FST, Heidelberg, Germany), titanium chamber frames were implanted to sandwich the extended double skin layer of the animal's back. One layer of skin was completely excised in a circular area of approximately 15 mm. The remaining skin layer, consisting of epidermis, subcutaneous tissue, and a striated skin muscle layer (panniculus carnosus), was covered with the second titanium frame (frame-to-frame distance: ca. 300µm) incorporating a coverslip (Fig. 1 A, B). Aseptic procedures were used for all surgical techniques. Following chamber implantation, the mice were kept in separate cages with free access to laboratory chow and water.

The microsurgical technique used for implantation of chambers was similar to that described previously. The dorsal skinfold chamber is feasible for long term investigations on various implants and allows direct visualization of the microcirculation and vascularization of implants [24, 25] (Fig. 2 A, B).

Implantation Procedure

Porous scaffolding matrices with three different pore diameters (1: <75 µm, 2: 75-212 µm, and 3: 250-300 µm) were under investigation. Discoid specimens (diameter ≈5 mm, thickness ≈300 µm) were punched from the copolymer film before implantation and used as dermis substitutes (Fig. 3 A, B).

To reduce the effects of immediate surgical trauma on the chamber skin tissue a recovery period of 48 hours between the implantation of skinfold chamber and copolymer scaffolding matrices was chosen. For implantation the mice were positioned into a special device and the coverslip was removed. The sterilized copolymer matrix implant was transferred onto the panniculus carnosus in the center of the chamber. The chamber was then filled with approx. 60µl of physiological sodium solution and closed using a new sterile coverslip. After that, the animals were placed in their cages.

Histological Preparation

After 7 (n = 9), 14 (n = 9), and 21 (n = 18) days the animals were sacrificed for histological examination by an intravenous overdose of pentobarbital (Narcoren Merial, Hallbermoos, Germany). The copolymer scaffolding matrices and adjacent skin tissue were removed en bloc, pinned onto a cork sheet and fixed in a 5.0% formaldehyde solution. The specimens were then divided, oriented and placed in a processing cassette, taken through a graded ethanol series, and embedded in paraffin for a complete edge-to-edge cross-sectional view of the implant disc. Semi-thin (≈5µm) tissue sections along with the copolymer matrix were obtained using a microtome. Sections were deparaffinized and standard stained with hematoxylin and eosin.

Light Microscopy

Copolymer scaffolding matrix was discriminated from surrounding tissue using polarized light and analyzed on days 7, 14, and 21 postimplantation. For quantitative assessment of multinucleated foreign body giant cells, two sections (thickness of the optical slide: 5 µm) from each of the 36 implants were evaluated by the same person, who at the time of analysis did not know which group and time point a specimen belonged to. Digital photographs of 2 AOF and 2 BOF (≈ 0.047 mm2) within each copolymer matrix section were captured at 400x magnification using a confocal light microscope (Axioskop, Zeiss) and a digital microscope camera (HV-C20M, Hitachi). The observation fields were randomly selected along the entire length of the sagittal implant section. Two basal fields near the skin-tissue/copolymer-matrix interface and

two apical fields from the areas bordering on the coverslip of the chamber were examined. Multinucleated foreign-body giant cells were identified and counted using computer-assistance (analySIS®, Soft Imaging System, Muenster, Germany).

Scanning Electron Microscopy (SEM)

For the examination by scanning electron microscope the formalin fixed specimens were dehydrated using an ethanol/water gradient. Dehydrated samples were dried at the critical point of CO_2 using a Balzers CPD 030. Samples were then mounted, gold coated in an Edwards S 150B sputter coater and examined with a Siemens SEM at 20 kV.

Image-analytical System AnalySIS®

A qualitative analysis of changes to the copolymer matrix integrity and quantification of matrix fragmentation were performed on digital scanning micrographs (400fold magnification) of each section within two basal and two apical observation fields. Evaluation via PC followed using analySIS® 3.0- image-analytical software (Soft Imaging System, Muenster, Germany). Digital microscope images were automatically calibrated by analySIS®: The software recognized the microscope magnification selected and automatically calibrated the images accordingly. Image-acquisition artifacts were corrected via filters and shading correction. Copolymer scaffolding matrix was differentiated from the surrounding fibrovascular tissue as well as from optically empty pore areas. Solid copolymer texture and copolymer matrix fragments were separated from the remaining image information via thresholds and morphological filters. Operations such as changing of the grey value, splitting of the brightness area or determination of threshold values for the creation of the binary image were determined for each image individually. The element distribution was emphasized by coloring (Fig. 4). Subsequently the color distribution pattern was analyzed and the entire area of biopolymer calculated automatically. The surface area of the solid copolymeric texture was expressed in percentage of the total area of the micrograph ($\approx 0.047 mm^2$). Evaluated data was saved, along with the acquired images, in the integrated, image-analytical database. All measurement data was automatically entered into a spreadsheet and statistically evaluated.

Statistical Analysis

Comparisons between the different groups and observation fields (basal vs. apical) were performed using Kruskal-Wallis analysis of variance on ranks. When significant differences were found, this nonparametric test was followed by the pair-wise multiple comparison procedure (Dunn's Method). Differences were considered significant when $p < 0.05$. All statistical calculations were performed with a commercially available software package (Sigma Stat, SPSS Inc., Version 2.03)

Results

On day 7 little stroma was present with few fibroblasts, leucocytes and macrophages located within the pores, but scattered throughout the entire scaffolding matrix (mostly concentrated in BOF). On day 14, the macrophages fused, amplified into multinucleated giant cells and migrated into the biomaterial. It was found that the phagocytes spread on the matrix surface and adhered themselves to the biomaterial. The majority of multinucleated phagocytes were found to be aligned along the skin-tissue/copolymer-matrix interface within the BOF. On day 21, giant cells, initially present only at the base of matrices, encompassed all areas of the matrices. A high number of giant cells was still counted especially in <75µm matrices within BOF (Fig. 5 A-D).The copolymer matrix of <75µm matrices was almost completely surrounded and engulfed by giant cells. The microscopical observation revealed that all matrices induced the development of cellular-fibrous tissue around the edges of the implant. This tissue was comprised primarily of fibroblasts, extracellular matrix, and leucocytes, and also contained some blood vessels. At day 14, superior vascularization of the granulation tissue surrounding the copolymer matrices at their edges, was observed. Also, a thin layer of tissue of similar composition covered the implants on their apical surface. Twenty-one days after implantation, 75-212µm and 250-300µm matrices were found to be embedded in well-vascularized connective tissue (Fig. 6).

The earliest signs of significant erosion and delamination of copolymer matrix surface were shown by the scanning electron microscopy on day 7 predominantly within the basal observation fields. On days 14 and 21 the loss of matrix structural integrity continued as a result of increased matrix fragmentation. Copolymer matrices with a pore size of < 75µm in particular were found to be excessively fragmented (Fig. 7). The fragmentation was accompanied by an increased accumulation of macrophages and foreign-body giant cells in the copolymer matrices, mainly visible in <75µm matrices. On day 21 implant fragments were also found intracellularly, incorporated by multinucleated phagocytic cells. Significant decreases of copolymer matrix area percentages within the basal and apical observation fields were already seen in implants of all types on day 14 postimplantation compared to the values calculated on day 7 (Fig. 8 A-C). The rate of matrix loss for 75-212µm and 250-300µm matrices was found to be lower than in <75µm matrices. Twenty-one days postimplantation, the <75µm implants had an average residual area percentage at the BOF of approximately 15%, which represents 68% of the original copolymer area on day 7. Image-analytical evaluation over the period of 21 days revealed a reduction of the copolymer matrix area by approximately 32% for the <75µm matrices, 23% for the 75-212µm matrices and 18% for the 250-300µm matrices. Identical changes within the percentage of implant area were determined for the AOF, where no significant differences were recognized compared to the values of BOF (data not shown). The analysis of matrix area changes suggested that on average 75% of the total lost matrix area (assuming that

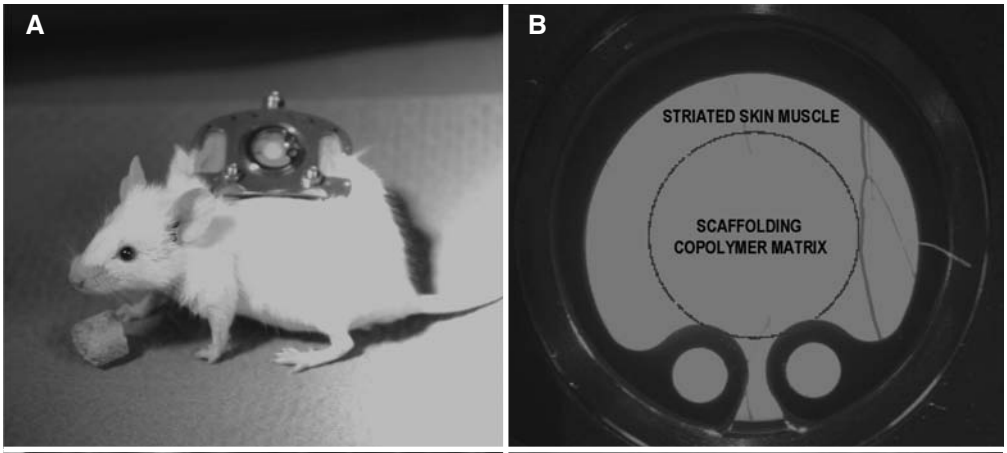

Fig. 1. A Balb/c mouse bearing a dorsal skinfold chamber. The mouse does not show signs of discomfort after surgery. B Copolymer matrix implanted in the center of observation window of the chamber. The implant directly contacts the striated skin muscle layer. The window is sealed by means of a sterile cover glass.

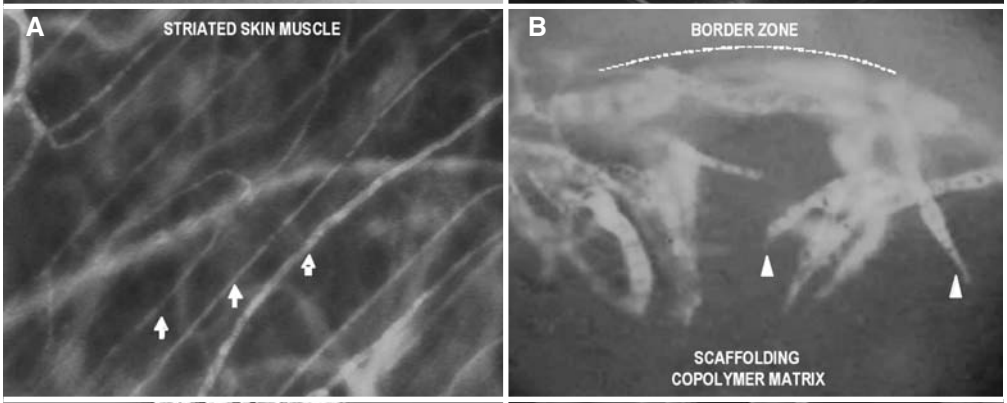

Fig. 2. The chamber model allows direct in vivo visualization of the microcirculation and angiogenesis. The intravital fluorescence images show (A) characteristic capillaries (arrows) of the skin muscle and (B) perfused blood vessel sprouts (triangles) in the border zone of scaffolding copolymer matrix two weeks after implantation.

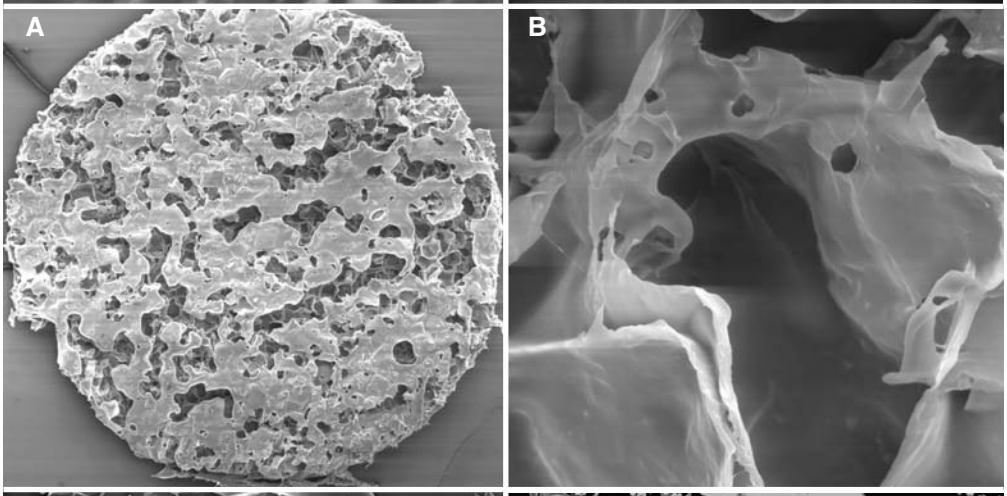

Fig. 3. Surface texture of the PEGT/PBT copolymer matrix (pore diameter: 75-212µm). A Dermal substitute as a discoid implant (magnification: 20fold) B Porous microstructure of the scaffolding matrix (magnification: 400fold).

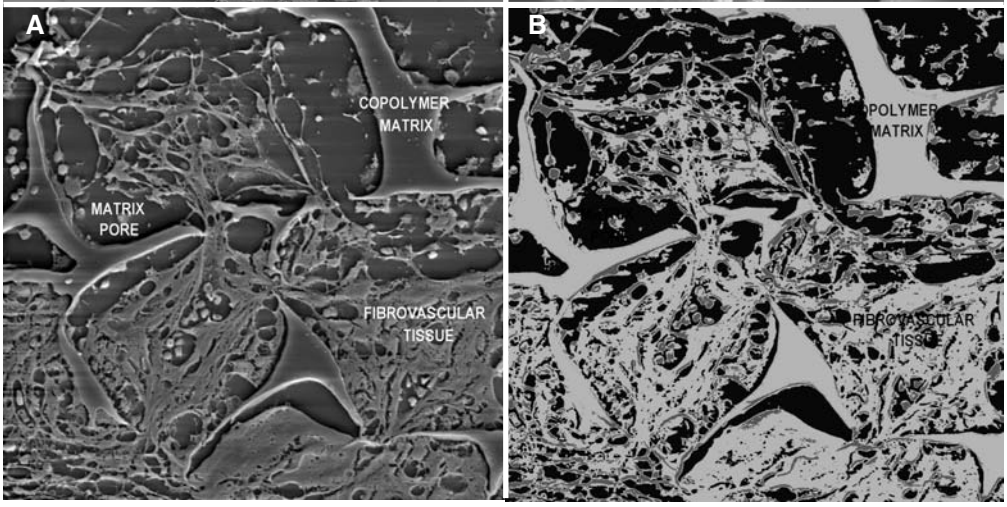

Fig. 4. A Scanning electron image of the basal observation field of 75-212µm copolymer matrix (magnification: 400fold). B The binary image of the observation field is emphasized by coloring. The copolymer matrix is separated from the remaining image information by analySIS®.

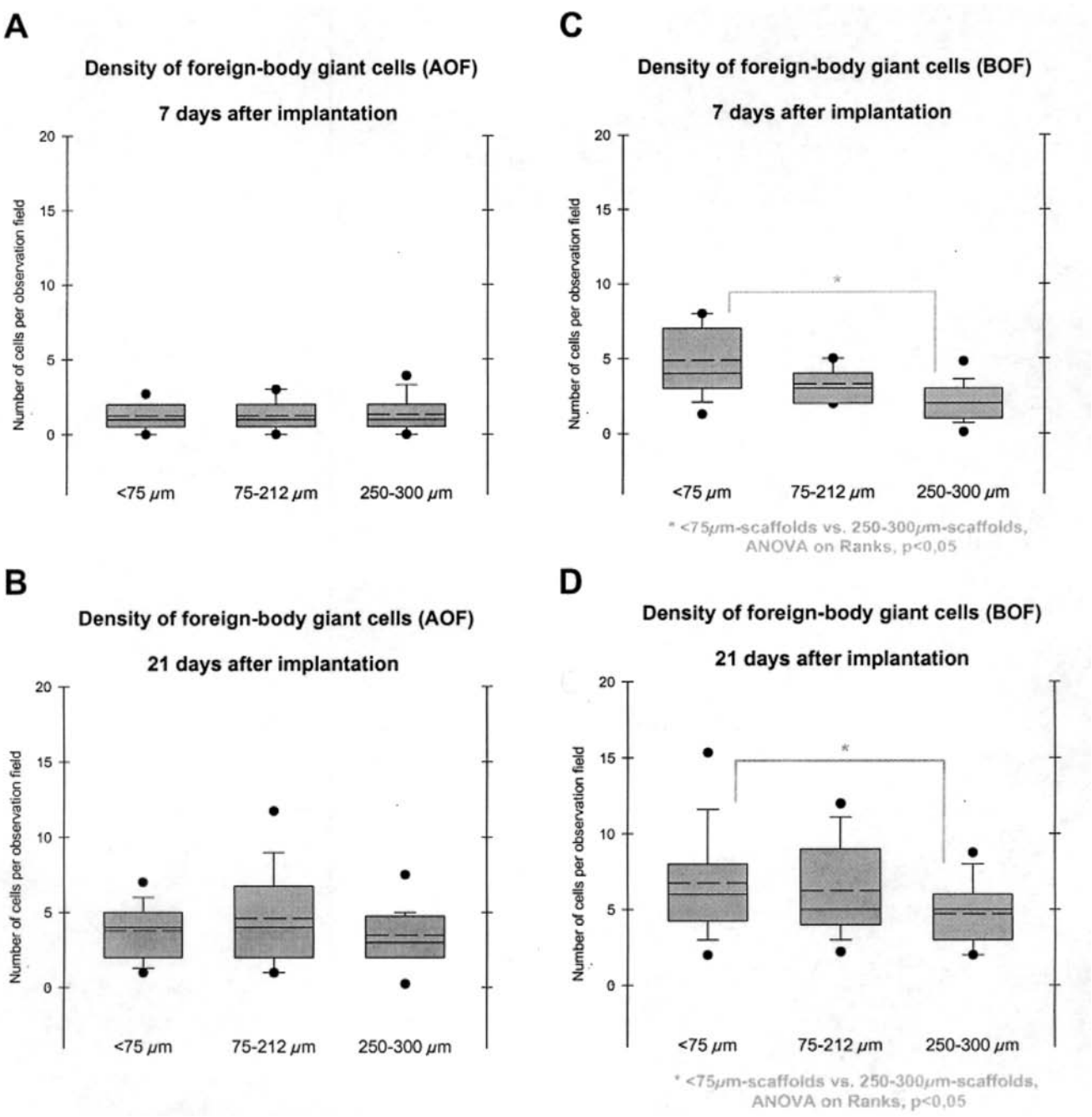

Fig. 5. The figure shows the density of foreign-body giant cells depending on scaffold type, observation field within the copolymer matrix (AOF vs. BOF) and timepoint after implantation. Box plots graph data as a box representing statistical values. The boundary of the box closest to zero indicates the 25th percentile, a line within the box marks the median, and the boundary of the box farthest from zero indicates the 75th percentile. Whiskers above and below the box indicate the 90th and 10th percentiles. The mean (long dash) and outlying data points beyond 5th and 95th percentiles are also graphed.

there was no significant copolymer loss during the first week after grafting) was degraded between days 7 and 14, and an additional 25% during the following week.

Discussion

The knowledge about the mechanisms of inflammatory response to an implanted synthetic biomaterial is still limited. Numerous factors are suspected to influence the intensity and character of the foreign-body reaction. The micromotion at the implant/host-tissue interface, which could differ due to varying surface textures because of different pore sizes, may have an influence on the inflammatory process. The inflammatory cells are known to produce various mediators, such as chemotactic, angiogenic and anti-angiogenic factors. The exposure of interfacial inflammatory cells, such as macrophages, to micro-shear stress can activate the release of such products, leading to inflammation and foreign body reaction [26, 27].

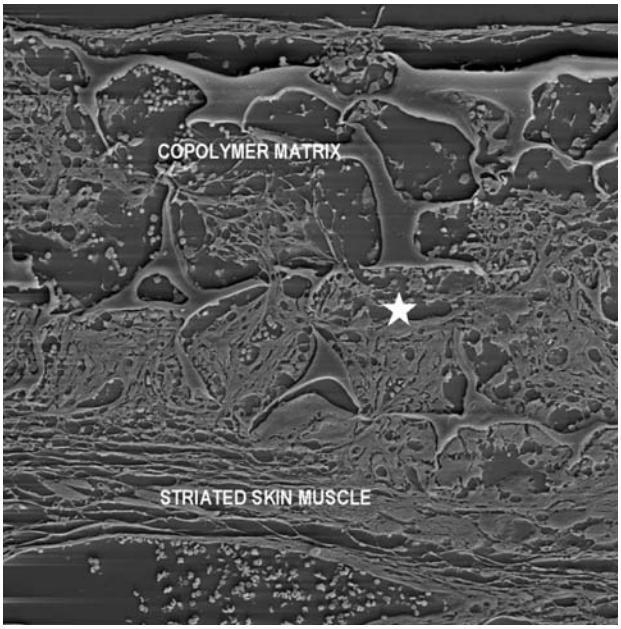

Fig. 6. Vascularized copolymer scaffolding matrix (Pore size: 75-212 µm) three weeks after implantation. Ingrown fibrovascular tissue is marked by white star (magnification: 200fold).

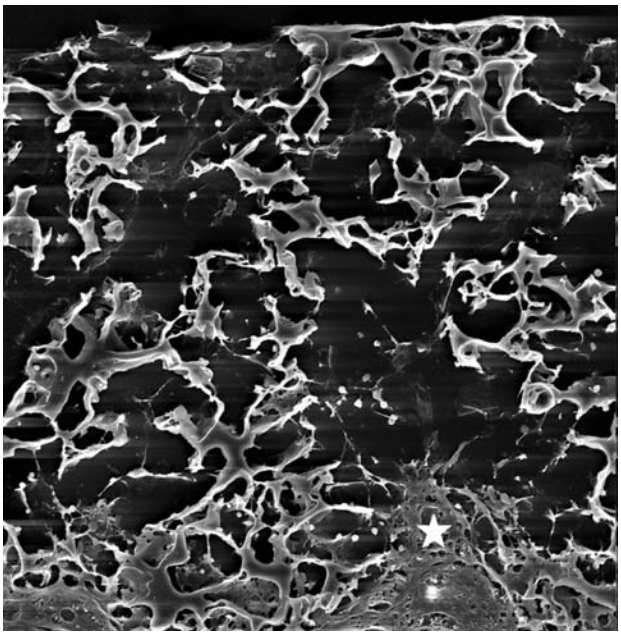

Fig. 7. Excessively fragmented matrix of copolymer scaffold with the pore size of <75 µm three weeks after implantation (magnification: 200fold). Only the basal observation field of the cross-section shows a minimal fibrovascular ingrowth (white star).

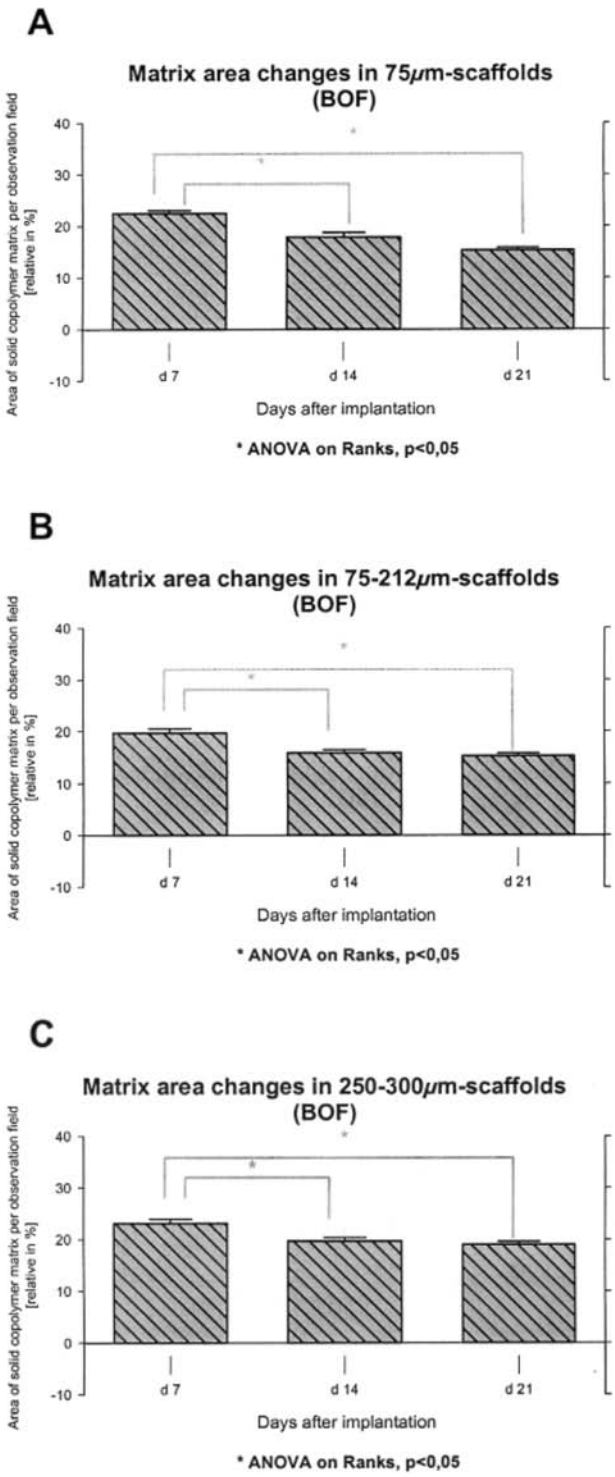

Fig. 8. Vertical bar charts demonstrate the quantity of copolymer matrix area detected by digital image analysis in percent per observation field. Significant reduction of copolymer matrix area within the basal observation fields (A-C) was found for all scaffolding matrix types on day 21 post implantation as compared to the values on day 7 post implantation.

In this work, the number of phagocytic cells increased constantly during the implantation time of the biomaterial matrix. Mononuclear macrophages and multinucleated foreign-body giant cells, some with intracellular matrix particles, were present at the implant-tissue interface and within the implant matrix. This suggests that the degradation of copolymer involves an intracellular elimination. Starting from day 14 of histological evaluation, all copolymer implants showed signs of foreign body inflammation, with a stronger expression in the copolymer matrices with the pore size of <75 µm (which were microscopically

found to be excessively fragmented). Simultaneously, matrices of this pore size showed low degrees of vascularization and connective tissue formation. As such, it seemed that the higher extent of vascularized fibrous tissue brings about protection from degradation. Degradation and absorption of the copolymer matrix occurred slowly in implants that underwent fibrous connective tissue infiltration at a much faster rate. On the other hand, it is possible that a potential accumulation of low-molecular degradation products within the degradable matrix may have disturbed a profound fibrovascular infiltration of the porous copolymer matrix. Accumulation of low-molecular breakdown products may hinder cell proliferation when the concentration of these products is high enough. Reports from in-vitro studies on absorbable polymers, intended to investigate the effects of degradation products on cell cultures, strengthen this assumption [28, 29]. It is possible that the biological conditions required for tissue regeneration within the implanted porous matrix may be altered by accumulation of copolymer decomposition products leading to inhibition of cell proliferation.

The attempt to quantify the degradation of biomaterial, was performed via the image-analytical software analySIS® on digital images from histological sections. Before calculating the changes of matrix area, it was hypothesized that a relative increase of matrix area would occur. It was thought that this would be due to the increased matrix fragmentation during the implantation period as detected by scanning electron microscopy. However, no increase in matrix area was demonstrated by analySIS®. On the contrary, the image analysis showed a progressive decrease of the matrix area during the 21 days following implantation. It was supposed that this was more likely caused by resorption of the biopolymer as well as being due to the intracellular incorporation of the fragmented implant particles by giant cells. Additionally, identification of small matrix fragments and separation of the copolymer matrix from the remaining image information, to create a binary image became more difficult due to the increased ingrowth of fibrovascular tissue during the implantation. It is also possible that progressive tissue infiltration of the porous copolymer matrix was able to cause contraction as well as expansion of the scaffolding matrix. These possible processes may have had a falsifying influence on the calculation of the real matrix area and do not correctly reflect the specific changes in degradation area. Another disadvantage of the applied method in quantifying the post-implantive matrix area changes results from ignoring the three-dimensional structure of the scaffolding matrices by analyzing images of the histological sections. Due to the irregular geometrical structure of the porous implants with inconstant diameter, form, density and distribution of pores, the presence of the copolymer mass within the observation fields was also inconstant. Because of this, we believe that the analySIS®-assisted method for calculation of the matrix area changes does not quantify the post-implantive biodegradative behaviour of PEGT/PBT copolymer matrices exactly, and therefore the results should be interpreted with care.

Conclusions

In this study, we quantified the biodegradation of PEGT/PBT-block-copolymer matrices by digital imaging analysis. The matrix degradation was evaluated in relation to the intensity of the host tissue response and the amount of fibrovascular tissue infiltration in the pores of the matrix. We showed that the structural differences of the porous scaffolds have had a varying impact on the degradative behavior in vivo. However, with the porous scaffolds we used, no controlled reduction or loss of the biopolymer approximately the same rate as required for replacement by the newly produced dermis-like tissue was demonstrated. It took three weeks before the complete dermis substitute of approximately 300 μm thickness was filled by a vascularized fibrous tissue. For a clinical application it may be too long, especially with regard to the risk of infection of the biomaterial due to poor vascularization.

Today, no synthetic biomaterial is available that exactly fulfills all of the requirements for an optimal dermis substitute. The ability of the biodegradable porous PEGT/PBT copolymer matrix to serve as dermis substitute is promising, but still remains to be evaluated in detail .

Acknowledgments: The authors acknowledge ISOTIS Inc, the Netherlands, for providing PEGT/PBT scaffolds for this study. The study was financially supported in part by ISOTIS Inc., the Vogelsang Foundation and Philoktet e.V., Bochum, Germany.

References

1. LaFrance, M.L. and D.W. Armstrong, Novel living skin replacement biotherapy approach for wounded skin tissues. Tissue Eng, 1999. 5(2): p. 153-70.
2. Heitland, A., et al., Update on the use of collagen/glycosaminoglycate skin substitute-six years of experiences with artificial skin in 15 German burn centers. Burns, 2004. 30(5): p. 471-5.
3. Wake, M.C., C.W. Patrick, Jr., and A.G. Mikos, Pore morphology effects on the fibrovascular tissue growth in porous polymer substrates. Cell Transplant, 1994. 3(4): p. 339-43.
4. Zeltinger, J., et al., Effect of pore size and void fraction on cellular adhesion, proliferation, and matrix deposition. Tissue Eng, 2001. 7(5): p. 557-72.
5. McGlohorn, J.B., et al., Evaluation of smooth muscle cell response using two types of porous polylactide scaffolds with differing pore topography. Tissue Eng, 2004. 10(3-4): p. 505-14.
6. Suh, H., M.J. Song, and Y.N. Park, Behavior of isolated rat oval cells in porous collagen scaffold. Tissue Eng, 2003. 9(3): p. 411-20.
7. Effah Kaufmann, E.A., P. Ducheyne, and I.M. Shapiro, Evaluation of osteoblast response to porous bioactive glass (45S5) substrates by RT-PCR analysis. Tissue Eng, 2000. 6(1): p. 19-28.
8. Adams, R.K., G.K. Hoeschele, and W.K. Witsiepe, Thermoplastic polyether ester elastomers, in Thermoplastic elastomers, H.E. Schroeder, Editor. 1996, Hansen Publishers: Munich. p. 191-225.
9. Harris, J.M., Introduction to biotechnical and biomedical applications of poly(ethylene glycol), in Poly(ethylene glycol) chemistry, biotechnical and biomedical applications, J. M. Harris, Editor. 1992, Plenum Press: New York. p. 1-12.

10. Kawai, F., Bacterial degradation of a new polyester, polyethylene glycol-phtalate polyester. J. Envirom. Polym. Degrad., 1996. 4 (1): p. 21-28.
11. Jun, H.S., et al., Synthesis of copolyesters containing poly(ethylene terephtalate) and poly(epsilon-caprolactone), and its biodegradability. Stud. Polym. Sci., 1994. 12: p. 498-504.
12. Witt, U., R.J. Muller, and W.D. Deckwer, Biodegradation of polyester copolymers containing aromatic compounds. J. Macromol. Sci.-Pure Appl. Chem., 1995. A32 (4): p. 851-856.
13. Bakker, D., et al., Biocompatibility of a polyether urethane, polypropylene oxide, and a polyether polyester copolymer. A qualitative and quantitative study of three alloplastic tympanic membrane materials in the rat middle ear. J Biomed Mater Res, 1990. 24(4): p. 489-515.
14. Beumer, G.J., et al., A new biodegradable matrix as part of a cell seeded skin substitute for the treatment of deep skin defects: a physico-chemical characterisation. Clin Mater, 1993. 14(1): p. 21-7.
15. Beumer, G.J., C.A. van Blitterswijk, and M. Ponec, Biocompatibility of a biodegradable matrix used as a skin substitute: an in vivo evaluation. J Biomed Mater Res, 1994. 28(5): p. 545-52.
16. Radder, A.M., H. Leenders, and C.A. van Blitterswijk, Interface reactions to PEO/PBT copolymers (Polyactive) after implantation in cortical bone. J Biomed Mater Res, 1994. 28(2): p. 141-51.
17. van Dijkhuizen-Radersma, R., et al., Biocompatibility and degradation of poly(ether-ester) microspheres: in vitro and in vivo evaluation. Biomaterials, 2002. 23(24): p. 4719-29.
18. Wang, H.J., et al., Engineering of a dermal equivalent: seeding and culturing fibroblasts in PEGT/PBT copolymer scaffolds. Tissue Eng, 2003. 9(5): p. 909-17.
19. van Dorp, A.G., et al., A modified culture system for epidermal cells for grafting purposes: an in vitro and in vivo study. Wound Repair Regen, 1999. 7(4): p. 214-25.
20. van Dorp, A.G., et al., Bilayered biodegradable poly(ethylene glycol)/poly(butylene terephthalate) copolymer (Polyactive) as substrate for human fibroblasts and keratinocytes. J Biomed Mater Res, 1999. 47(3): p. 292-300.
21. El-Ghalbzouri, A., et al., The use of PEGT/PBT as a dermal scaffold for skin tissue engineering. Biomaterials, 2004. 25(15): p. 2987-96.
22. Deschamps, A.A., et al., Design of segmented poly(ether ester) materials and structures for the tissue engineering of bone. J Control Release, 2002. 78(1-3): p. 175-86.
23. Claase, M.B., et al., Porous PEOT/PBT scaffolds for bone tissue engineering: preparation, characterization, and in vitro bone marrow cell culturing. J Biomed Mater Res A, 2003. 64(2): p. 291-300.
24. Druecke, D., et al., Neovascularization of poly(ether ester) block-copolymer scaffolds in vivo: long-term investigations using intravital fluorescent microscopy. J Biomed Mater Res, 2004. 68A(1): p. 10-8.
25. Steinstraesser, L., et al., The human host defense peptide LL37/hCAP accelerates angiogenesis in PEGT/PBT biopolymers. Ann Plast Surg, 2006. 56: p. 93-98.
26. Patel, J.D., et al., Inhibition of bacterial and leukocyte adhesion under shear stress conditions by material surface chemistry. J Biomater Sci Polym Ed, 2003. 14(3): p. 279-95.
27. Shive, M.S., et al., Shear stress and material surface effects on adherent human monocyte apoptosis. J Biomed Mater Res, 2002. 60(1): p. 148-58.
28. Ignatius, A.A. and L.E. Claes, In vitro biocompatibility of bioresorbable polymers: poly(L, DL-lactide) and poly(L-lactide-co-glycolide). Biomaterials, 1996. 17(8): p. 831-9.
29. Taylor, M.S., et al., Six bioabsorbable polymers: in vitro acute toxicity of accumulated degradation products. J Appl Biomater, 1994. 5(2): p. 151-7.

Received: April 30, 2006 / Accepted: August 31, 2006

Address for correspondence:
Stefan Langer, MD
Dept. of Plastic & Hand Surgery, Burn Center
University Hospital Bergmannsheil
Ruhr University Bochum
Buerkle-de-la-Camp Platz 1
D-44789 Bochum, Germany
Tel.: +49 234/302-3426
Fax: +49 234/302-6379
Email: stefan.langer@ruhr-uni-bochum.de